

## Floppy Modes in Crystalline and Amorphous Silicates

Martin T. Dove,<sup>1</sup> Mark J. Harris,<sup>2</sup> Alex C. Hannon,<sup>2</sup> John M. Parker,<sup>3</sup> Ian P. Swainson,<sup>4</sup> and Manoj Gambhir<sup>1,5</sup>

<sup>1</sup>*Mineral Physics Group, Department of Earth Sciences, University of Cambridge, Downing Street, Cambridge, CB2 3EQ, United Kingdom*

<sup>2</sup>*ISIS Facility, Rutherford Appleton Laboratory, Chilton, Didcot, Oxfordshire, OX11 0QX, United Kingdom*

<sup>3</sup>*Department of Engineering Materials, Sheffield University, Mappin Street, Sheffield, S1 3JD, United Kingdom*

<sup>4</sup>*Neutron and Condensed Matter Science Branch, AECL Research, Chalk River Laboratories, Chalk River, Ontario, K0J 1J0, Canada*

<sup>5</sup>*Cavendish Laboratories, University of Cambridge, Madingley Road, Cambridge, CB3 0HE, United Kingdom*

(Received 21 August 1996)

We present the results of comparative inelastic neutron scattering measurements of both amorphous and crystalline silicates. We demonstrate the presence of floppy modes in amorphous silica and potassium disilicate over the energy scale 0–5 meV. A peak is also observed at 5 meV in amorphous silica, which is traditionally associated with the boson peak. By comparison with the spectrum of crystalline  $\alpha$ -cristobalite, we show that it, in fact, arises from the transverse acoustic modes. The same peak in amorphous potassium disilicate cannot be resolved because it is obscured by a large number of floppy modes. [S0031-9007(96)02212-0]

PACS numbers: 61.12.-q, 61.43.Fs, 63.20.Dj, 63.50.+x

Our conceptual understanding of the microscopic nature of the excitations observed in amorphous systems is poor compared to those of crystalline materials. This is especially true of the low-energy excitations that are observed between, say, 0–10 meV [1]. Sound propagates through glasses, and so well-defined longitudinal phonons are stable at relatively short wave vectors (less than  $1 \text{ \AA}^{-1}$ ) [2]. However, it is not clear how far the phonon picture can be applied to the excitations that occur at moderate wave vectors (between, say,  $2\text{--}4 \text{ \AA}^{-1}$ ). Two features of the low-energy excitation spectrum that are particularly interesting in this respect are the so-called floppy modes [3] and the boson peak [4]. Floppy modes are low-energy deformations of a structure composed of linked “rigid” structural units such as  $\text{SiO}_4$  tetrahedra. The floppy modes can propagate with these units rotating against each other without distorting. The boson peak is a feature that is found in the Raman scattering spectra of many glasses at about 5 meV and which obeys Bose-Einstein statistics. However, it is not seen in the Raman spectra of corresponding crystalline phases. It has been assigned various mechanisms in the past, sometimes linked with the floppy modes, as we discuss below. There are a number of other unusual properties of glasses, such as the linear temperature dependence of the specific heat at very low temperatures and the low-temperature plateau in the thermal conductivity. These properties are usually thought to be associated with the existence of low-energy excitations, particularly if they enable the system to behave as a two-level system.

Buchenau *et al.* [5] have demonstrated that acoustic waves coexist with another kind of harmonic excitation below about 4 meV in vitreous silica, and suggested that these extra modes mainly involve rotations of the  $\text{SiO}_4$  tetrahedra as rigid bodies, essentially behaving as floppy

modes. This picture serves as a guide for the nature of the excess modes at energies lower than the boson peak (which is at about 5 meV in vitreous silica), but the implication is that the origin of the boson peak could be explained by the existence of floppy modes. Elliott [6] more recently suggested that the boson peak may arise from phonon scattering caused by density fluctuations at the medium length scale. In this model the phonons are localized within domains of structural units surrounded by voids. An increase in the vibrational density of states,  $g(E)$ , results from those phonons which have a mean free path commensurate with the domain size. The (quasi)harmonicity of the model provides a trivial basis for the temperature dependence of the intensity of the boson peak.

Other models tend to provide expressions for the potential energy from which good fits to specific heat and thermal conductivity data may follow. For example, the “soft potential model” [7] specifically gives a form for the potential energy that encourages tunneling at low temperatures and harmonic motion at higher temperatures, but gives little illumination as to the configurational variables that experience these potential wells. Most of the models that attempt to explain the boson peak depend upon a certain degree of medium-range order which supports the existence of low-frequency acoustic modes.

In this Letter, we present comparative neutron scattering measurements of the low-energy dynamics of both amorphous and crystalline silicates, because recent experimental and theoretical work on crystalline silicates has brought a new perspective to this issue [8]. We discuss the vibrational spectra of crystalline  $\alpha$ -cristobalite (the low-temperature polymorph of cristobalite,  $\text{SiO}_2$ , with tetragonal symmetry), vitreous silica ( $\text{SiO}_2$ ), and amorphous potassium disilicate ( $\text{K}_2\text{O}\cdot 2\text{SiO}_2$ ). We point out

certain striking similarities between them which provide a simple physical explanation for the boson peak, and establish the energy scale of the floppy modes.

The number of floppy modes in a system of linked rigid units (in this case,  $\text{SiO}_4$  or  $\text{AlO}_4$  tetrahedra) is given by a balance between the total number of degrees of freedom,  $F$ , and the number of constraints,  $C$ , that arise from the topology of the structure; the number of floppy modes is equal to  $F - C$  (of the total, six will correspond to the uniform translations and rotations of the structure) [3]. For a system of tetrahedra, linked at their vertices,  $F = 6$  per tetrahedron. For any pair of linked vertices there are three constraint equations: If  $\mathbf{r}_1$  is the position of the vertex of one unit, and  $\mathbf{r}_2$  is the position of the vertex of the linked unit, the constraints arise from  $\mathbf{r}_1 = \mathbf{r}_2$ . Thus, for the system of linked tetrahedra,  $C = 6$  per unit when all vertices are linked. With this simple way of counting, *there should be no floppy modes in a fully linked silicate crystal or glass*. To generalize to a silicate glass with  $n$  bridging bonds per tetrahedron,  $C = 3n/2$ . For example, for a potassium-disilicate glass  $\text{K}_2\text{O} \cdot 2\text{SiO}_2$ ,  $n = 3$  and the number of floppy modes is  $F - C = 1.5$  per tetrahedron. By comparison, there will be 16.5 vibrational modes per tetrahedron.

The major insight given by the recent analysis of floppy modes in crystalline silicates is that symmetry can have a major effect in reducing the number of *independent* constraints per tetrahedron (i.e., constraints become degenerate). The reasons for this have been documented elsewhere [8]. For relatively dense crystalline silicates, such as quartz and cristobalite, the floppy modes can exist over lines or planes of wave vectors. In less dense silicates, such as sodalite or zeolites, there can be more than one floppy mode for every wave vector. On the other hand, the change of symmetry at a displacive phase transition can reduce the number of floppy modes in the low-symmetry phases. This principle is clearly seen at work in cristobalite, where there are six planes of floppy modes in reciprocal space in the high-temperature cubic phase, but only a few lines of floppy modes in the low-temperature tetragonal phase. Inelastic neutron scattering measurements on a polycrystalline sample clearly show the reduction in the number of floppy modes on cooling through the phase transition [9]. This work shows that the energy scale for floppy modes is about 0–5 meV. A similar energy scale was found for the modes in the crystalline aluminosilicate leucite,  $\text{KAlSi}_2\text{O}_6$ , using inelastic neutron scattering from a single crystal [10]. The floppy modes in crystalline silicates have been called “rigid unit modes” (RUMs), which is a useful term since it denotes a special class of floppy modes. The existence of RUMs in crystalline silicates has been most convincingly demonstrated by electron diffraction measurements on cristobalite [11] and tridymite [12]: Streaks of diffuse scattering are observed which correspond to the intersections of planes of RUMs with the plane of reciprocal

space under observation. Most striking of all was the observation of curved surfaces of RUMs in tridymite [12].

Given the existence of a significant and measurable number of RUMs in crystalline silicates, we again address the issue of the existence of floppy modes in amorphous silicates, taking account of the energy scale suggested by inelastic neutron scattering experiments. In our measurements we used high-purity powdered samples of crystalline  $\alpha$ -cristobalite, amorphous silica, and amorphous potassium disilicate,  $\text{K}_2\text{O} \cdot 2\text{SiO}_2$ . The sample of  $\alpha$ -cristobalite was chosen because our previous analysis has shown that, unlike high-temperature  $\beta$ -cristobalite (cubic), there are very few RUMs present [8,9], which sets a lower bound for comparison with amorphous silica. By contrast, the simple method of counting constraints and degrees of freedom suggests that there should be many floppy modes in amorphous potassium disilicate. This sets an upper bound against which we can compare the low-energy vibrational spectrum of amorphous silica. Similar data have been collected for  $\alpha$ -cristobalite and amorphous silica by other workers [13], but improved source and instrument characteristics enabled us to obtain improvements over previous data sets. In our opinion, neutron scattering has an advantage over Raman scattering when we compare crystalline and amorphous samples, since the selection rules for Raman scattering are quite different in the two types of materials, whereas inelastic neutron scattering will give the vibrational density of states in both cases.

The present data were obtained with the samples at ambient conditions, using the PRISMA spectrometer at the ISIS spallation neutron source [14]. PRISMA is an indirect geometry time-of-flight spectrometer. It has an array of 16 independent scattering arms, spaced at  $2^\circ 2\theta$  from each other, each consisting of a pyrolytic graphite analyzer and a detector. The analyzer/detector arms were all set to measure scattered neutrons with an energy of 14 meV, and a number of settings of the whole detector arm were measured, so that the total range in wave-vector transfer,  $Q$ , covered was from 2.0 to 3.6  $\text{\AA}^{-1}$ . The energy resolution was approximately 0.5 meV at zero-energy transfer. The spectra were normalized against standard vanadium scans and merged using in-house software. The spectra from the background and empty sample can were subtracted, and the data were corrected for the effects of multiple scattering and normalized against the different masses of the samples. The resultant spectra were then scaled by the population factor,  $n(E) + 1$ , and scaled by  $1/E$ , to give a quantity proportional to  $g(E)/E^2$ . The final spectra are shown in Fig. 1.

It will be useful to compare the neutron scattering measurements with a calculation of the one-phonon density of states in  $\alpha$ -cristobalite. This was performed using a well-tested empirical model potential [15] for  $\text{SiO}_2$ , and the dynamical matrix was diagonalized for 8000 points over a grid in one octant of the Brillouin zone. For comparison

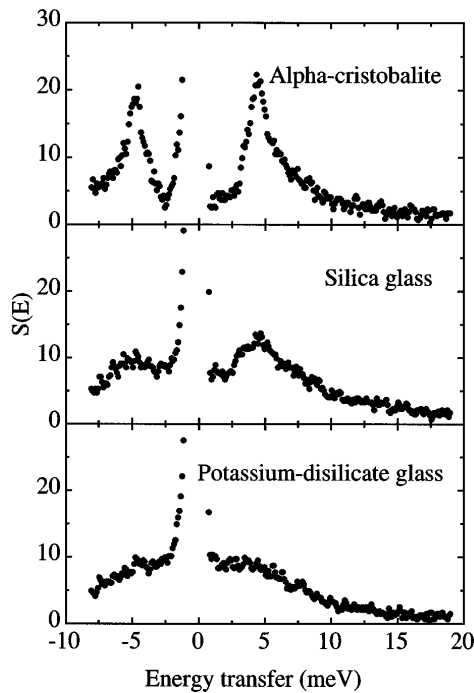


FIG. 1. Inelastic neutron scattering spectra for  $\alpha$ -cristobalite, amorphous silica, and amorphous potassium disilicate, corrected for the background and factors such as multiple scattering, and reduced to a form proportional to  $g(E)/E^2$ .

with experiment we have weighted the calculation by the factor  $1/E^2$ . No account has been taken of the different neutron scattering lengths for Si and O, but we note that these are probably not significantly different for the purposes of comparison with experiment. The calculations are shown in Fig. 2, together with the phonon dispersion curves along symmetry directions. One point that should be noted is that the lowest two phonon branches along [110] are the only two RUMs in  $\alpha$ -cristobalite [8,9], and these are at lower frequencies than the phonon branches along the other symmetry directions. What should also

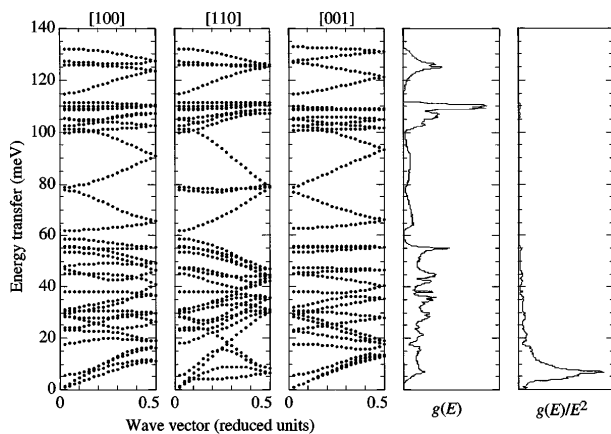


FIG. 2. Calculated  $g(E)$  and  $g(E)/E^2$ , together with phonon dispersion curves along symmetry directions, for  $\alpha$ -cristobalite.

be noted is that there is not likely to be any orientational disorder of the  $\text{SiO}_4$  tetrahedra in  $\alpha$ -cristobalite like that found in  $\beta$ -cristobalite [9,16]. In the latter case, the orientational disorder arises from the simultaneous excitation of whole planes of RUMs in reciprocal space [8,9], which can cause the tetrahedra to rotate by an average angle of  $17^\circ$  from their “average” orientations. This disorder leads to a broad distribution of RUM frequencies [9]. In  $\alpha$ -cristobalite it is more likely that the two RUM branches will have relatively sharp frequencies.

*First, we compare the neutron data for  $\alpha$ -cristobalite with the calculated density of states.* The agreement is very good. The important feature to note is that there is a peak at 5 meV in both experiment and calculation, which tails off more slowly at higher energies. This peak arises from the transverse acoustic branches in all directions, and from the RUM branches along [110], although the latter only contribute to the sharp component seen at the top of the peak. This can be seen in the calculated phonon dispersion curves shown in Fig. 2.

*Second, we compare the spectra for  $\alpha$ -cristobalite and amorphous silica.* It should be noted that the phonon peak at 5 meV in  $\alpha$ -cristobalite is also seen in amorphous silica, although slightly broadened. In amorphous silica this peak is the feature usually associated with the boson peak. The data immediately suggest that the boson peak in amorphous silica arises from the same motions as the corresponding peak in  $\alpha$ -cristobalite, and thus is largely made up from the transverse acoustic modes.

*Third, we focus our comparison between the spectra of  $\alpha$ -cristobalite and amorphous silica on the low energy regime, between 0–5 meV.* Although slight, it is clear that there is an increased number of low-energy modes in amorphous silica. This suggests the existence of a larger number of low-energy floppy modes in amorphous silica with a broad energy distribution, similar to the RUMs observed in  $\beta$ -cristobalite [9] and leucite [10]. The presence of an increased number of low-energy modes in amorphous silica is rather surprising in light of the balance between the constraints and degrees of freedom discussed above. There are two possible solutions. One is that amorphous silica contains a significant (although not necessarily large) number of nonbridging Si-O bonds, which could arise from the presence of defects or surfaces. The existence of nonbridging bonds will lead to a net reduction in the number of constraints. The second possibility is that there is some “hidden symmetry” that allows some of the constraints to become degenerate or near degenerate. This might arise from the existence of large open rings of linked  $\text{SiO}_4$  tetrahedra, for example, although the presence of large rings alone, without the additional effects of symmetry, cannot break the basic balance between constraints and degrees of freedom.

It is worth noting that a recent determination of the pair distribution functions for  $\alpha$ - and  $\beta$ -cristobalite, from measurements of the neutron scattering function  $S(Q)$ , has

shown that over the length scale 5–10 Å  $\beta$ -cristobalite is more like amorphous silica than  $\alpha$ -cristobalite [16]. The floppy modes in  $\beta$ -cristobalite are in part broad because of the dynamic disorder. In amorphous silica there is static disorder rather than dynamic disorder, but at an instantaneous point in time the disorder in both cases leads to very similar medium-range structure. Thus we expect any floppy modes in amorphous silica to be broad in energy as in  $\beta$ -cristobalite [9], rather than sharp as in  $\alpha$ -cristobalite.

Fourth, we compare the spectra for amorphous silica and amorphous potassium disilicate, particularly in the energy range 0–5 meV. In the latter spectra there is an enhanced population of the vibrational modes with energies between 0–5 meV, so much so that the boson peak at about 5 meV is obscured and can only be identified by comparison with amorphous silica. This result was of course expected from the fact that there is a greater number of degrees of freedom than there are constraints that arise from nonbridging Si-O bonds, but the important quantitative point is that the floppy modes span the energy range 0–5 meV. This is fully consistent with the results for crystalline  $\beta$ -cristobalite [9] and leucite [10]. This is also consistent with our point that the energy scale for the floppy modes is just below the energy of the boson peak. Incidentally, the way the floppy modes “hide” the boson peak in this case is also seen in  $\text{Ge}_x\text{Se}_{1-x}$  chalcogenide glasses for  $x \leq 0.2$  [17]. The Se-rich materials are more floppy [3], and the boson peak seen in the more rigid structures (e.g.,  $x = \frac{1}{3}$ ) is then hidden beneath a broad distribution of floppy modes.

In conclusion, our results have established the energy scale of 0–5 meV for floppy modes in amorphous silicates. The peak seen at 5 meV, which is conventionally called the boson peak, is associated with the same motions as the transverse acoustic modes in crystalline silicates. Many more floppy modes are seen in the potassium disilicate glass owing to the existence of nonbridging oxygen atoms (one per tetrahedron) leading to an underconstrained network of linked tetrahedra. But the fact that there is clearly a number of floppy modes in the range 0–5 meV in the pure silica glass is a counterexample to the simple counting scheme for the balance between constraints and degrees of freedom.

We are grateful to the EPSRC for financial support.

---

[1] F. Terki, C. Levelut, M. Boissier, and J. Pelous, Phys. Rev. B **53**, 2411 (1996); M. Foret, E. Courtens, R. Vacher,

and J. B. Suck, Phys. Rev. Lett. **77**, 3831 (1996).  
 [2] C. Masciovecchio, G. Ruocco, F. Sette, M. Krisch, R. Verbeni, U. Bergmann, and M. Soltwisch, Phys. Rev. Lett. **76**, 3356 (1996).  
 [3] Y. Cai and M.F. Thorpe, Phys. Rev. B **40**, 10535 (1989); W.A. Kamitakahara, R.L. Cappelletti, P. Boolchand, B. Halfpap, F. Gompf, D.A. Neumann, and H. Mutka, Phys. Rev. B **44**, 94 (1991); M.F. Thorpe, J. Non-Cryst. Solids **57**, 355 (1983); S.W. Deleeuw, H. He, and M.F. Thorpe, Solid State Commun. **56**, 343 (1985).  
 [4] F.J. Bermejo, A. Criado, and J.L. Martinez, Phys. Lett. A **195**, 236 (1994).  
 [5] U. Buchenau, M. Prager, N. Nücker, A.J. Dianoux, N. Ahmad, and W.A. Phillips, Phys. Rev. B **34**, 5665 (1986); U. Buchenau, H.M. Zhou, N. Nücker, K.S. Gilroy, and W.A. Phillips, Phys. Rev. Lett. **60**, 1318 (1988).  
 [6] S.R. Elliott, Europhys. Lett. **19**, 201 (1992).  
 [7] V.G. Karpov, M.I. Klinger, and F.N. Ignatiev, Sov. Phys. JETP **57**, 439 (1987); H.R. Schober, Physica (Amsterdam) **201A**, 14 (1993).  
 [8] M.T. Dove, in Amorphous Insulators and Semiconductors: Proceedings of NATO ASIS, edited by M.F. Thorpe and M.I. Mitkova (Kluwer, Dordrecht, to be published); M.T. Dove, A.P. Giddy, and V. Heine, Trans. Am. Crystallogr. Assoc. **27**, 65 (1991); M.T. Dove, A.P. Giddy, and V. Heine, Ferroelectrics **136**, 33 (1992); A.P. Giddy, M.T. Dove, G.S. Pawley, and V. Heine, Acta Crystallogr. A **49**, 697 (1993); K.D. Hammonds, M.T. Dove, A.P. Giddy, V. Heine, and B. Winkler, Am. Mineral. **81**, 1057 (1996); M.T. Dove, V. Heine, and K.D. Hammonds, Mineral. Mag. **59**, 629 (1995).  
 [9] I.P. Swainson and M.T. Dove, Phys. Rev. Lett. **71**, 193 (1993); J. Phys. Condens. Matter **7**, 1771 (1995).  
 [10] H. Boysen, in Phase Transitions In Ferroelastic And Co-Elastic Crystals, edited by E.K.H. Salje (Cambridge University Press, Cambridge, England, 1990), pp. 334–349.  
 [11] G.L. Hua, T.R. Welberry, R.L. Withers, and J.G. Thompson, J. Appl. Crystallogr. **21**, 458 (1988).  
 [12] M.T. Dove, K.D. Hammonds, V. Heine, R.L. Withers, Y. Xiao, and R.J. Kirkpatrick, Phys. Chem. Miner. **23**, 55 (1996).  
 [13] A.J. Leadbetter, J. Chem. Phys. **51**, 779 (1969).  
 [14] U. Steigenberger, M. Hagen, R. Caciuffo, C. Petrillo, F. Cilloco, and F. Sachetti, Nucl. Instrum. Methods Phys. Res., Sect. B **53**, 87 (1991).  
 [15] M.J. Sanders, M. Leslie, and C.R.A. Catlow, J. Chem. Soc. Chem. Commun. 1271 (1984).  
 [16] M.T. Dove, D.A. Keen, A.C. Hannon, and I.P. Swainson, Phys. Chem. Miner. (to be published).  
 [17] S. Sugai, Phys. Rev. B **35**, 1345 (1987).